JOURNAL OF SOLID STATE CHEMISTRY 96, 31–47 (1992)

Synthesis of Novel Compounds with the Pyrochlore and Hexagonal Tungsten Bronze Structures

KENNETH P. REIS, A. RAMANAN, AND
M. STANLEY WHITTINGHAM

Department of Chemistry and Materials Research Center, State University of New York at Binghamton, Binghamton, New York 13902-6000

Received July 29, 1991

Low-temperature hydrothermal synthesis of acidified tungstate solutions leads to the formation of defect pyrochlores, $MW_2O_6O_{1/2} \cdot xH_2O$, and compounds with the hexagonal tungsten bronze (HTB) structure, $M_xWO_{3+x/2}$, where M is normally a monovalent cation. The initial pH of the tungstate solution is critical to the structure obtained; a pH of 3.5 leads to the formation of a pyrochlore phase and pH 1.5 gives the hexagonal tungsten bronze structure. The HTB compound is formed with lithium or sodium in the hexagonal tunnel whereas the pyrochlore contains sodium, cesium, or rubidium inside the three-dimensional tunnels. Both phases are metastable and decompose around 500°C. The sodium ions in the pyrochlore phase can be exchanged for many monovalent cations and those in the hexagonal phase by hydrogen. Both structures readily intercalate lithium.

Introduction

The tungsten oxides and their intercalated products $M_xWO_{3+x/2}$ have been extensively studied over the years because of their electrochemical and electronic properties, which make them attractive as active electrodes in electrochromic displays (*1*). Their structures permit the ready insertion of cations such as hydrogen, lithium, and sodium. However, the kinetics of these reactions have been insufficient to allow for their use in active displays such as those required in watches, calculators, and computer screens. Recently, new interest has revolved around their use in large-scale static displays such as windows, mirrors, and sunglasses.

Important to the kinetics of the insertion reaction and its reversibility is the crystalline structure of the tungsten oxides. The WO_6 octahedral building blocks join at the corners, which results in a variety of crystalline structures. In an effort to synthesize new compounds with interesting structural and ionic properties, we have employed a variety of low-temperature techniques. These techniques include mild hydrothermal synthesis, ion exchange, and chemical insertion reactions at ambient temperatures, e.g. using *n*-butyl lithium to lithiate a compound. These low-temperature synthetic techniques allow for the formation of novel compounds that cannot be synthesized by traditional high-temperature solid-state reactions.

Recently, we reported preliminary results on the hydrothermal synthesis and characterization of two novel sodium tungstates with the pyrochlore and hexagonal tungsten

0022-4596/92 $3.00

bronze (HTB) structure (*2, 3*). The incorporation of sodium inside the tunnels of these structures is of interest, since sodium is too small to stabilize the framework at higher temperatures. For the pyrochlore phase, this is the first report of an alkali-inserted tungsten pyrochlore with tungsten as the only transition metal. Further, both compounds contain unusually large amounts of water and, for the HTB phase, more than can be accommodated by the structure. In this paper, we report the formation of various tungstates by hydrothermal synthesis, the ion-exchange properties, and their intercalation chemistry. We also discuss the thermal stability of these phases.

Experimental

$Na_2WO_4 \cdot 2H_2O$ was obtained from Aldrich Chemical. All other M_2WO_4 (M = Li, Cs, Rb) materials were prepared by the solid-state reaction of WO_3 and M_2CO_3 in the stoichiometric amounts following established procedure.

In a typical experiment, 20 ml of 1 M $Na_2WO_4 \cdot 2H_2O$ solution was acidified at room temperature with the required amount of 1 N HCl to give pH values of approximately 1.5 and 3.5. The solutions were heated at 155°C and autogeneous pressure (about 5 atm) for 3 days in Parr 4745 stainless steel acid digestion reactors. Since prolonged standing at low pH led to a precipitate, the solutions were sealed and heated within 1 hr of preparation. The microcrystalline white product was filtered, washed with ethanol, and dried in air. For M = Li and Na the acidified solution was clear, but for M = Rb, Cs, and K a white insoluble precipitate formed around pH 5.5. The precipitate is amorphous to X-ray diffraction.

The ion-exchange reactions were accomplished by using 1 molar solutions of the metal nitrate, MNO_3 (M = K, Rb, Cs, NH_4, H, Ag), and heating at 80°C for a few hours to a week, with the larger cations taking the most time. Silver is exchanged for sodium quite easily at room temperature. Addition of silver nitrate to Na-pyrochlore leads immediately to Ag-pyrochlore, which is yellow. Exchange with hydrogen is accomplished by using 1 M HNO_3 and exchanging the solution every hour for about 5 hrs. Care must be taken, as the pyrochlore phase will decompose if the temperature is above 80°C or if it is heated longer than 1 hr (*4*).

Sodium and lithium content were determined by atomic absorption (Perkin–Elmer). The compounds were dissolved in 0.3 M $K_3Fe(CN)_6$ in 4% KOH solution. Li_2WO_4 and Na_2WO_4 were used as the standards. The ammonia content was determined by Kjeldahl's method, which involves heating the compound in aqueous NaOH and collecting the evolved ammonia gas in 0.1 N HCl. Titration of the acid solution with a standard NaOH solution gave the ammonia content.

Thermal gravimetric analysis was performed on a Perkin–Elmer TGA7 in an inert atmosphere (N_2 or He) at 1°C/min. Differential scanning calorimetry was run on a Perkin–Elmer DSC7 under N_2. The scanning rate was 10K/min. X-ray powder diffraction was performed on a Rigaku/Siemens diffractometer at 1° of 2θ/min and lattice parameters were determined by a least-squares analysis.

Lithium intercalation was accomplished by reaction with n-butyllithium (1.6 M) obtained from Aldrich Chemical. The concentration of the stock solution of n-butyllithium, after reaction with isopropyl alcohol and dilution with water, was determined prior to each reaction by titration with a standard HCl solution. The samples were heated under vacuum to drive off the water of hydration prior to lithiation. The maximum lithium content was obtained by adding an excess of n-butyllithium (between 4–5 ml) to 100–300 mg of sample at room temperature under nitrogen. The color of the

solids changed from white to blue to blue-black to black depending on the degree of reduction. The reactions seem to occur very rapidly, usually in just a few minutes. However, the mixture was allowed to stand overnight under nitrogen to ensure completion of the reaction. The sample was filtered and washed with hexane. The amount of unreacted lithium was determined by back-titration, which gave the degree of lithiation. The lithium content of some samples was also determined by atomic absorption as a cross check.

Results and Discussion

Hydrothermal synthesis of acidified alkali tungstates allowed us to prepare both the pyrochlore and hexagonal structures with alkali cations incorporated inside the tunnels of these compounds. Powder X-ray diffraction studies (Fig. 1) of the sodium samples showed that two distinct white phases were formed depending on the initial pH of the acidified solution. For pH 3.5–4.5, the patterns could be completely indexed on a cubic pyrochlore-type lattice with a = 10.333(2) Å. A hexagonal phase was formed for pH 1.3–2.0 with cell parameters of a = 7.311(4) and c = 2*3.895(2) Å. Intermediate pH values gave a mixture of the cubic and hexagonal phases, and a pH of less than 1.0 gave a mixture of unidentified phases believed to be tungstic acids, while pH values above 5.0 yield no precipitate. The best yields were obtained for pH 3.5 and 1.5 for the cubic and hexagonal phases, respectively.

Atomic absorption and TGA were used to determine the composition of the hexagonal and pyrochlore compounds. The compositions were $Li_{0.20}WO_{3.10} \cdot 0.5H_2O$ and $Na_{0.26}WO_{3.13} \cdot 0.5H_2O$ for the hexagonal tungsten bronze structure. The lithium and sodium contents were typical of the HTB structure. The chemical analysis of the cubic phase showed it was a defect pyrochlore with the composition $Na_{1.1}W_2O_{6.55} \cdot 1.4H_2O$. SEM ruled out the presence of chlorine in either phase, but sodium could barely be detected, much less quantified, by this technique.

The pyrochlore and hexagonal tungsten bronze structures possess a rigid tungsten–oxygen framework built up of layers containing distorted corner shared WO_6 octahedra (Fig. 2) and arranged to form six-membered rings. In hexagonal WO_3, the layers are stacked along the [001] plane, giving one-dimensional tunnels. In cubic pyrochlore WO_3, the layers are linked along the [111] direction to form interconnected three-dimensional tunnels. These tungstates provide an interesting set to study the effect of structure on chemical reactivity and physical properties. In addition, these two structures allow for the determination of openness of structure on chemical behavior. The pyrochlore structure has expanded about 26% above that of the simple perovskite WO_3,which is itself a relatively open structure being a distorted perovskite, ABO_3, with all A sites vacant.

Our original compounds (*2*) were synthesized in pyrex tubes. After we changed to the Parr acid digestion reactors, we found a slight rhombohedral distortion (Fig. 3) of the pyrochlore with α = 90.3°; the hexagonal parameters are a = 7.445(2) Å and c = 17.90(5) Å. Changing the pH and/or temperature or heating time had no effect on the degree of distortion. The distorted pyrochlore showed an identical water loss and decomposed into the same products as the cubic pyrochlore.

Closer examination of the X-ray powder diffraction patterns of the pyrochlore phases obtained from the pyrex tubes showed that there was a slight asymmetry of the peaks that would be expected to split upon a rhombohedral distortion. All lattice parameters reported in this paper will be based on the cubic cell. The reason for this is that the distortion is small and, upon ion exchange

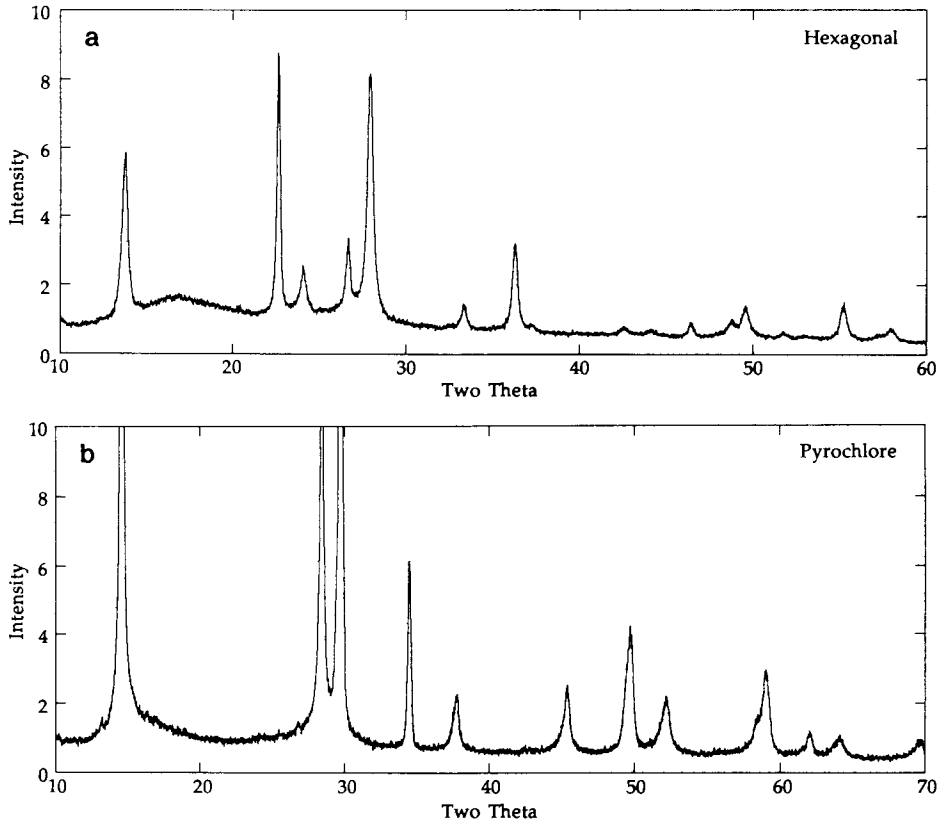

FIG. 1. X-ray powder diffraction patterns of (a) hexagonal tungsten bronze and (b) sodium cubic pyrochlore phases.

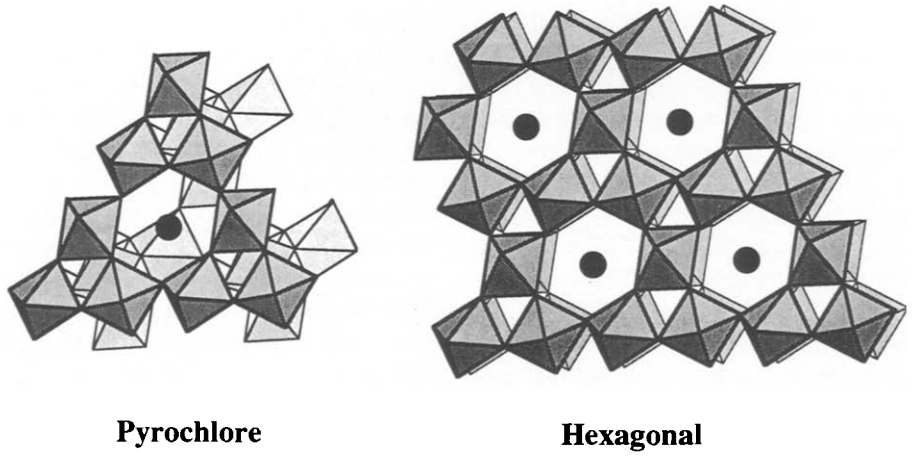

FIG. 2. Structures of pyrochlore and hexagonal tungsten bronzes phases.

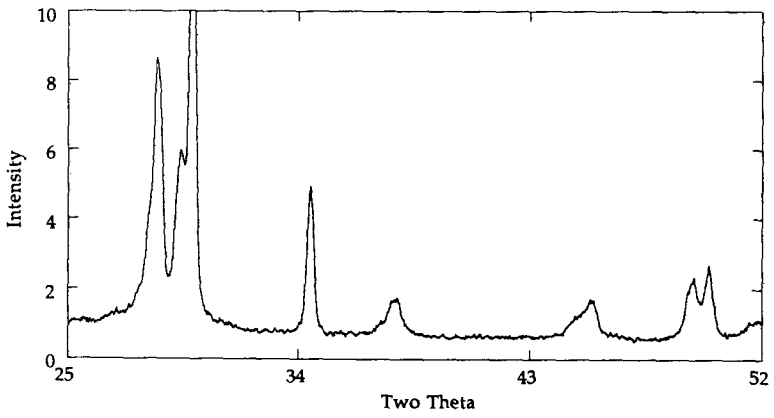

FIG. 3. X-ray powder diffraction pattern of the rhombohedrally distorted sodium pyrochlore phase.

or chemical insertion, the crystallinity of the phase decreases, which makes it difficult to index the pyrochlore on the rhombohedral cell due to the increased broadness of the peaks.

The full oxide pyrochlore stoichiometry is $M_2B_2O_6O'$. The ideal pyrochlore structure is cubic with the space group $Fd3m$. The M, B, and O′ ions occupy the special positions 16*d*, 16*c*, and 8*b*, respectively. The oxygens reside on the 48*f* site. Defect pyrochlores AB_2X_6, originally discovered by Babel *et al.*(*5*), are ideally cubic. These pyrochlores are defective at both the 16*d* and 8*b* sites. Over the years, there have been numerous reports that many of the defect pyrochlores deviate from the cubic symmetry. Sleight *et al.*(*6*) showed that $ANbWO_6$ (A = Tl, Rb) phases were tetragonal, and they attributed this to the statistical occupancy of Nb and W on the octahedral sites. Pyrochlores of the type ANb_2O_5F (A = Cs, Tl) are triclinic though the distortion is small (*7*). The defect pyrochlores, $Pb_2Ru_2O_{6.5}$ and $PbTlNb_2O_{6.5}$, were shown to deviate from the $Fd3m$ space group because of oxygen vacancy ordering and ordering of Pb and Tl on the A sites (*8*). Rhombohedrally distorted pyrochlores have also been reported in the literature (*9*).

It is not yet clear why the pyrochlore shows a rhombohedral distortion. A neutron diffraction study did not show the expected distortion (*10*), probably due to the large coherent scattering of hydrogen which led to a high background. On-going studies (*11*) on a deuterated sample with improved peak-to-background ratio also are not showing any rhombohedral distortion.

Tungstic acid is the term applied to various solids precipitated from tungstate solutions by strong acids. The solids precipitated from these solutions depend upon the reaction conditions. Understanding why different structures are formed depending on the initial pH of the solution involves a number of parameters, the first of which is the solution chemistry of tungsten. Isopolytungstates are formed upon acidification of the tungstate, WO_4^{2-}, solution. Due to the difficulty of isolating crystalline salts, the structural studies of what anions could be present in solution are limited, and this system is not well understood. The study of aqueous polytungstate equilibria is hindered by the extreme range of rates observed. Some of the rates of formation of the isopolytungstates are slow, and the equilibrium might not be reached for several weeks. On the other hand, some reactions are unusually fast, being completed in 10^{-2} sec (*12*).

TABLE I

HYDROTHERMAL SYNTHESIS OF ALKALI TUNGSTATES

M_2WO_4	Pyrochlore(Å)	Hexagonal(Å)
Li	not formed	a = 7.300(2), c = 7.719(9)
Na	a = 10.333(2)	a = 7.311(4), c = 7.778(3)
K	not formed	not formed
Rb	a = 10.173(2)	too few peaks to index
Cs	a = 10.299(9)	—

Therefore, it is very difficult to determine what polymeric species are in solution.

Since we reacted our solutions within an hour of preparation, we will discuss only those species that might be formed during that time. The discussion will be limited to the species probably present before reaction, because little work has been done involving temperature and pressure. At low pH values (<1.7), there are a number of isopolytungstates that could be present in solution, and small changes in pH affects the equilibrium. During our study, we took care to always have the initial pH at 1.5 ± 0.09. At this value a metatungstate is formed immediately upon acidification. This species is metastable and slowly transforms to tungstate-X $[H_2W_{12}O_{40}]^{6-}$. Upon prolonged standing, α-$[H_2W_{12}O_{40}]^{6-}$ is formed, which is the thermodynamically stable product. Despite the fact that incremental changes in pH affect the equilibrium, all pH values between 1.3–2.0 gave the hexagonal structure. At pH 3.5, the only probable species is $[H_7W_7O_{24}]^{2-}$ (*12*).

The cation plays an important role in these types of reactions. As seen from Table I, we have had mixed results using various alkali tungstates. Sodium and rubidium are the only cations that form both phases. Lithium forms a hexagonal phase but is probably too small to stabilize the pyrochlore phase, because we obtain no product above pH 3.0. Cesium forms the pyrochlore phase, though the compound is not well crystallized.

Apparently, it is the combination of the cation and polymeric species in solution that determines the phase formed. The pH of the solution controls the amount of sodium present in the reaction. Hydrothermal conditions facilitate the reaction at 155°C. Water gives a pressure of about 5 atm at this temperature. This slight pressure decreases the solubility of the product, and the cation acts as a template for the precipitation of the compounds. Though the initial pH is critical in determining the desired product, the pH of the solution after the reaction is 5.5 and 6.5 for the hexagonal and pyrochlore phases, respectively. Attempts at forming the compounds by starting with tungstic acid and making basic with NaOH to the appropriate pH values did not lead to the desired products. This is probably due to the irreversible formation of a variety of polymeric species at the start of the reaction.

Hexagonal Phase

As seen from Table I, hydrothermal synthesis of M_2WO_4 solutions (M = Li, Na, Rb) at pH 1.5 led to the formation of a phase that had the hexagonal tungsten bronze structure. All these compounds incorporated the respective metal ion into the hexagonal tunnels. The hexagonal tungsten bronze structure was originally described by Magnéli (*13*). He placed the metal ion in the center of the hexagonal tunnel; studies since then have shown that the ion is displaced

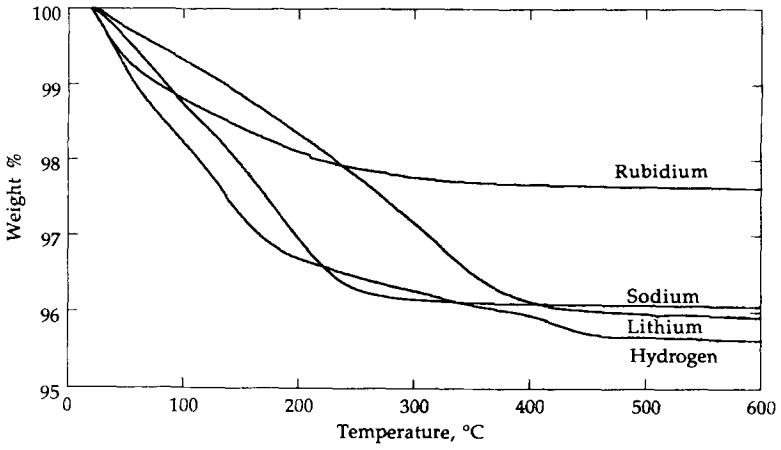

FIG. 4. TGA of hydrothermally prepared hexagonal phases.

slightly above the center of the cavity. Only the largest of cations (K, Rb, Cs, Tl, NH_4) have been known to form the hexagonal structure. Lithium and sodium are of particular interest because they are not known to form the hexagonal phase under ambient pressure conditions; however, they have been synthesized under intense pressure of 3000 and 65 atm, respectively (*14, 15*). The sodium content was not determined for these reaction conditions, which were considerably more rigorous than the synthesis reported here. Hexagonal WO_3 with empty tunnels has been prepared from the dehydration of $WO_3 \cdot \frac{1}{3}H_2O$ (*4*) and the oxidation of ammonium tungsten bronze by hydrogen peroxide (*16*). These same research groups have intercalated the smaller cations into hexagonal-WO_3 at room temperature. Unlike the intercalated compounds or the bronzes synthesized under extreme pressures, the compounds reported here are completely oxidized so that both metal and oxygen ions reside in the hexagonal tunnel.

As can be seen from the composition, the water content ($0.5H_2O/W$) is similar for both the lithium and sodium phases. The water content is higher than can be accommodated by the structure. A similar discrepancy was noted in $WO_3 \cdot \frac{1}{3}H_2O$ and was attributed to adsorbed water (*17*). TGA (Fig. 4) shows that water loss is dependent upon the cation incorporated inside the structure. If the water is only adsorbed on the surface, the dehydration temperatures and the weight losses should be similar. Therefore, it appears that some (if not all) of the water might be inside the tunnel along with oxygen and sodium. Location of all the ions is now being determined by powder neutron diffraction data (*10, 11*).

The Na-hexagonal phase is a metastable phase that irreversibly decomposes around 500°C into $Na_2W_4O_{13}$ and WO_3. Differential scanning calorimetry (Fig. 5) showed two peaks. The endotherm at 410 K (137°C) corresponds to the evolution of water, and the exotherm at 800 K (527°C) is the decomposition of the phase. The dehydration temperature is similar to the zeolitic water in $FeF_3 \cdot \frac{1}{3}H_2O$ whose structure is analogous to the HTB structure (*18*). The enthalpy changes are 10 kcal/mol for the evolution of water and 1.5 kcal/mol for the decomposition of the phase. The energy needed to remove the water from the lattice is similar to the value for uncoordinated water found in vermiculite (*19*). The small value of ΔH for the de-

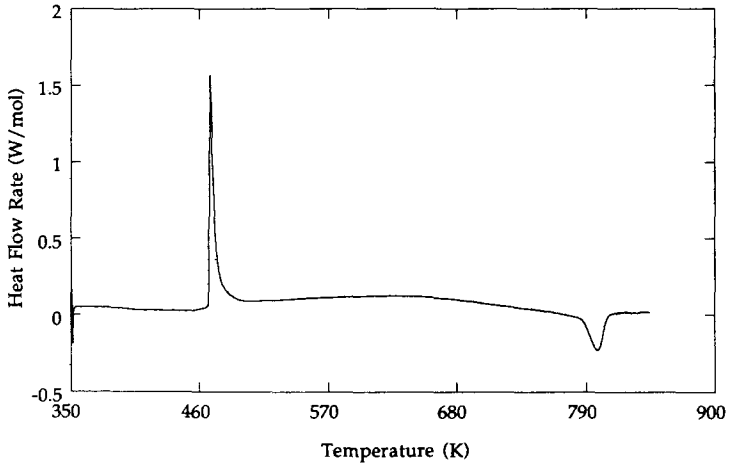

FIG. 5. DSC of sodium hexagonal tungsten bronze phase at 10 K/min.

composition can be attributed to the fact that the two structures, $Na_2W_4O_{13}$ and WO_3, are built up of the same WO_6 octahedra as in the HTB structure but with different arrangements. The value of the enthalpy change for the sodium hexagonal phase is higher than that found for hexagonal WO_3 with empty tunnels. Dickens and Kay (*20*) obtained a value of 0.5 kcal/mol and Susic and Solonin (*21*) determined that the value was 0.8 kcal/mol for the transformation from hexagonal to monoclinic WO_3. The enthalpy change and the temperature for the decomposition is slightly higher than hexagonal WO_3, which is attributed to sodium stabilizing the phase slightly. The temperature is relatively high due to the large activation energy needed for the breaking of W–O bonds and their rearrangement in the WO_3 framework while transforming to the new structures.

The sodium in the hexagonal structure can be exchanged for hydrogen, but the ion-exchange is quite difficult to achieve. It is accomplished by exchanging with 5 *M* HNO_3 at 80°C from several days to 2 weeks depending upon the sample. The diffusion is slow and can be attributed to the one-dimensional tunnels being partially blocked. This blockage can be overcome by grinding the sample thoroughly before exchanging and every 2 to 3 days after that until the reaction is completed. On every sample that was not ground, we obtained incomplete exchange of sodium for hydrogen.

The lattice parameters for hydrogen HTB are a = 7.327(2) Å and c = 7.779(4) Å, which are comparable to those of the sodium phase, a = 7.311(4) and c = 7.778(2) Å. Hexagonal WO_3 with empty tunnels can be prepared by heating to approximately 500°C with the lattice parameters being a = 7.289(2) Å, c = 7.775(4) Å. These parameters (Table II) are similar to those reported

TABLE II

LATTICE PARAMETERS OF THE HEXAGONAL PHASE OF WO_3

a(Å)	c(Å)	Volume/ W (Å^3)	Reference
7.298(3)	7.798(3)	59.95	(*4*)
7.323(6)	7.810(3)	60.45	(*16*)
7.291(8)	7.789(8)	59.76	(*22*)
7.289(2)	7.775(4)	59.62	This work

by other groups. Hexagonal WO_3 is stable to 500°C, where it decomposes into the thermodynamically stable monoclinic WO_3. No trace of sodium-containing species was found.

If the exchange for sodium is complete, the approximate composition would be $H_{0.26}WO_{3.13} \cdot 0.5H_2O$. TGA (Fig. 4) shows that there are two types of water in the structure and that the observed weight loss agrees with the reactions $H_{0.26}WO_{3.13} \cdot 0.5H_2O \rightarrow H_{0.26}WO_{3.13} \rightarrow WO_3$. The first step occurs from ambient to approximately 270°C, while the second step continues to approximately 475°C.

Pyrochlore Phase

Hydrothermal reactions of acidified M_2WO_4 (M = Na, Rb, Cs) tungstates at pH 3.5 led to the formation of a pyrochlore phase. All these compounds incorporated the alkali metal inside the three-dimensional tunnels. Several groups have reported the formation of $WO_3 \cdot xH_2O$ pyrochlore (*23–25*). Rubidium and cesium tungsten pyrochlores have been prepared via a high-temperature route, though little information was given (*25, 26*). Sodium-intercalated pyrochlore is unusual because normally larger size cations are needed to stabilize this phase. These pyrochlores incorporate water into the three-dimensional tunnels in contrast to the high-temperature analogs.

TGA (Fig. 6) shows that the water content is dependent upon the size of the cation. The smaller the cation, the greater the amount of water hydrated to it. This was also noted in the $ANbWO_6$ (A = Na, K) pyrochlores (*27*). As can be seen from Table I, the lattice parameters do not increase linearly with increasing size of cation incorporated inside the structure. The lattice parameter of cesium is larger than rubidium, which is expected, but sodium is larger than either phase. A similar discrepancy was observed for the $ANbWO_6$ pyrochlores. A possible reason for this discrepancy is that sodium occupies a different site in the structure than either rubidium or cesium. Previous studies have shown that rubidium and cesium prefer to occupy the larger 8*b* site, whereas sodium is on the smaller 16*d* site. Since the 8*b* site is slightly oversized for these cations, the structure contracts as much as possible.

Critical to the use of materials such as these sodium tungstates in electrochromic cells are their redox and ion-exchange properties. Pyrochlores have been reported to readily undergo ion exchange (*28*). For the pyrochlore structure synthesized here, sodium is exchanged for many monovalent cations (Table III), indicative of the rapid ionic mobility of the sodium ions within the lattice.

Ion-exchange reactions allow for the formation of novel pyrochlores that cannot be synthesized otherwise, either hydrothermally or at high temperature. Lithium appears to be the only monovalent cation that cannot be exchanged for sodium, though lithium has been incorporated into other pyrochlores by ion exchange (*29*). Silver, which is easily polarized, will exchange with sodium within seconds at room temperature. Addition of silver nitrate to Na-pyrochlore leads immediately to a color change from white to yellow, which indicates the rapid mobility of Ag in the pyrochlore structure. This compound holds promise as a good ionic conductor. Rubidium and cesium ion exchange very slowly (approximately 1 week) for sodium, which is due to their larger sizes. Unlike the $ANbWO_6$ pyrochlores (*27*), cesium and rubidium hydrate some water, as shown by the TGA. A previous report on WO_3 pyrochlore stated that cesium would not exchange for hydrogen (*25*).

There does not appear to be a simple correlation between the size of the monovalent cation and the lattice parameters of the pyrochlores (Table III). Thus, although the unit-cell size increases linearly from sodium through potassium to cesium with increas-

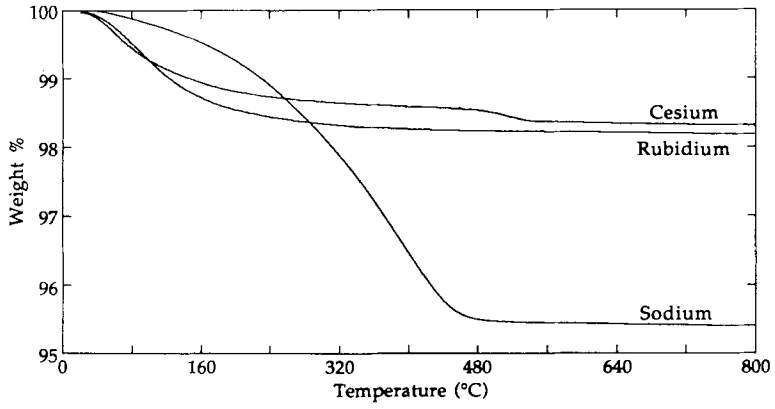

FIG. 6. TGA of pyrochlores prepared hydrothermally.

ing radius of the cation, rubidium and thallium do not follow this trend. This seems to suggest that the cations sit on different sites inside the structure. The possible locations for the cations to reside in the pyrochlore structure are the 8*b*, 16*d*, and 32*e* positions. The 8*b* site resides in the center of the cavity formed by the intersecting hexagonal tunnels. The 16*d* positions reside around the 8*b* site. There are two possible locations for the 32*e* site, either between the 8*b* and 16*d* positions or opposite the 16*d* site. Intensity calculations were performed to determine the possible locations of the various cations (Tl, Rb, Cs,K, Na, Ag) incorporated into the pyrochlore structure. The water molecules were placed on the 32*e* positions, and the intensity calculations were performed with the various cations occupying the 8*b* or 16*d* positions. Figures 7 and 8 show the variation of peak intensity with respect to the scattering factor of the incorporated cation. Cations that reside on the 16*d* position always have the {222} reflection as the strongest line, with the {111} and {311} reflection about equal but decreasing with increasing scattering potential. The X-ray powder diffraction pattern of Na-pyrochlore (Fig. 1) agrees with the calculated pattern with sodium on the 16*d* site, i.e., $I_{222} > I_{111} > I_{311} > I_{400} > I_{220}$. Silver and potassium, according to intensity calculations, also reside on the 16*d* position. The largest cations, Rb, Cs, and Tl, would be expected to occupy the largest site, which is the 8*b* position. Intensity calculations show that the {331} reflection is the strongest line in these cases, with the {220} reflection increasing with increasing scattering potential. X-ray powder diffraction patterns for Rb, Cs, and Tl have the {331} reflection as the strongest line and have a {220} reflection, indicating that these larger cations prefer the 8*b* position. The size of the unit cell can now be correlated

TABLE III

ION-EXCHANGED PYROCHLORES

Cation	Lattice parameter (Å)	Cell volume/W (Å^3)
Hydrogen	10.278(2)	67.86
empty	10.240(1)	67.10
Potassium	10.393(5)	70.16
Rubidium	10.320(4)	68.69
Cesium	10.410(5)	70.51
Silver	10.419(8)	70.69
Ammonium	10.344(5)	69.17
Thallium	10.317(8)	68.63

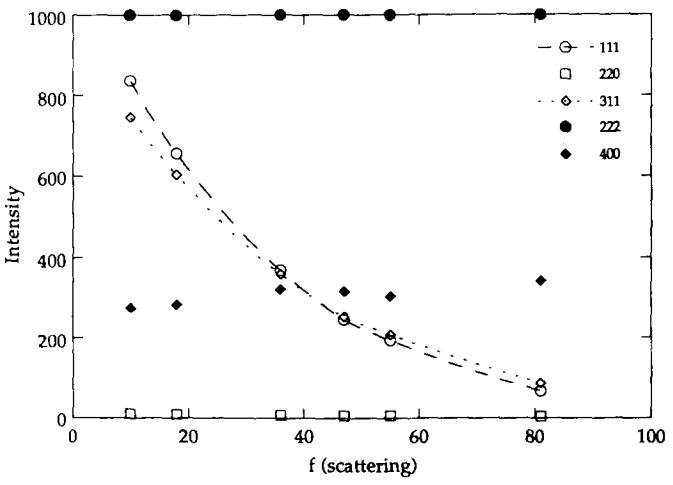

FIG. 7. Intensity calculations of pyrochlores as a function of scattering power of incorporated cation (Na, K, Ag, Rb, Cs, Tl) on the 16*d* site.

with the ionic radius of the inserted cation; as shown in Fig. 9, this correlation depends strongly on the position of the cation, with a smaller lattice being found for ions (H_3O^+, NH_4^+, Rb^+, Tl^+, and Cs^+) residing in the center of the tunnel.

The compounds formed by ion exchange show the same trends (Fig. 10) for water content and loss as the hydrothermally prepared pyrochlores. The larger cations coordinate less water than the smaller cations. The smaller cation will bind the water more strongly than the larger cation. Sodium loses its water completely at 350°C, potassium loses its water at 250°C, and thallium has very little water. The TGA (Fig. 11) of ammonium shows the evolution of water, then ammonium. Infrared showed an absorption

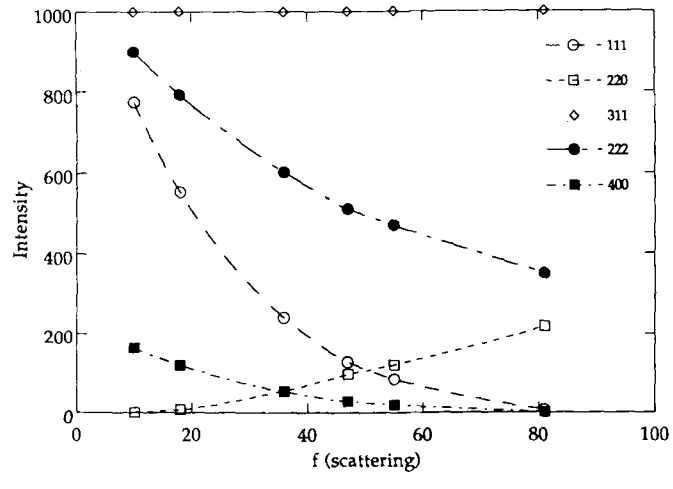

FIG. 8. Intensity calculations of pyrochlores with the cations on the 8*b* position.

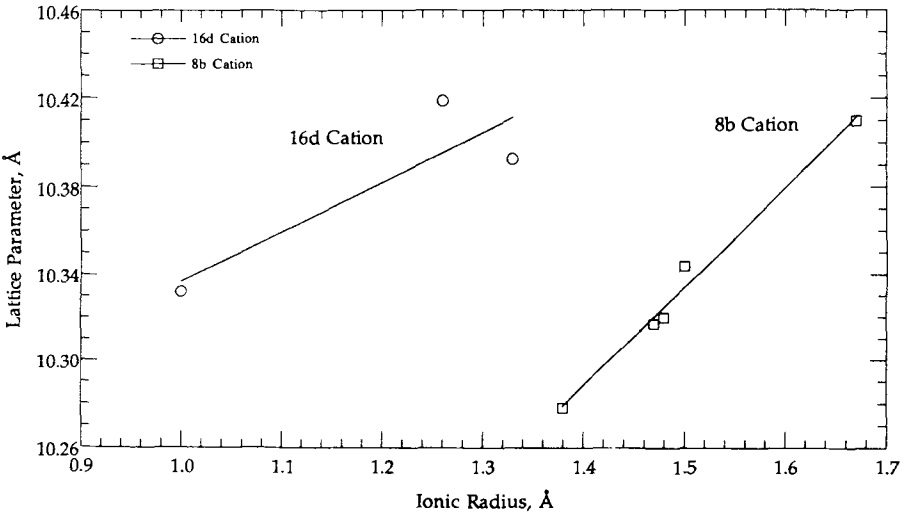

FIG. 9. Correlation between the unit cell size and the cation position and ionic radius in the ion-exchangd pyrochlores.

at 1400 cm^{-1}, which is indicative of the NH_4^+ ion. The ammonia content was determined by Keldjal's method to be 0.5 NH_4^+/W.

Pyrochlore $WO_3 \cdot xH_2O$ was prepared by exchanging the sodium for hydrogen. TGA shows that all the water is evolved by 300°C. By heating to this temperature, we were able to obtain pyrochlore-WO_3 with empty tunnels; it has the lattice parameter a = 10.2395(9) Å. Pyrochlore WO_3 is stable until 400°C, where it decomposes to the thermodynamically stable monoclinic WO_3.

The water content in our compounds is slightly greater than that in previous reports on WO_3 pyrochlore. Two groups (*24, 25*) reported approximately 0.5 H_2O/W, and we

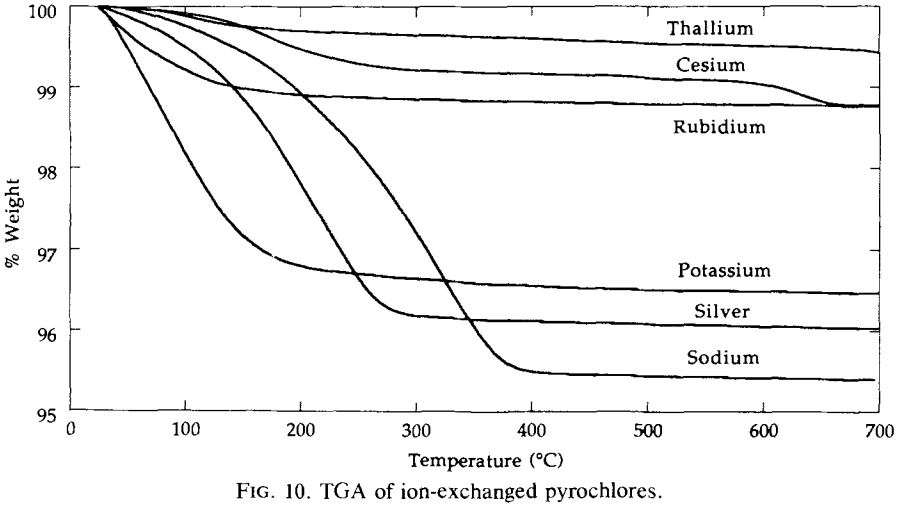

FIG. 10. TGA of ion-exchanged pyrochlores.

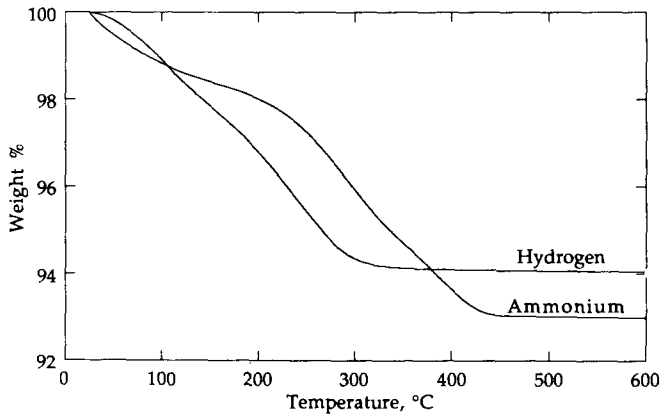

FIG. 11. TGA of ammonium and hydrogen pyrochlore prepared by ion exchange.

obtained 0.7 H_2O/W. A fourth group (*23*) reporting the synthesis of pyrochlore indicated the presence of water but gave no content. The pyrochlore compounds synthesized here will reabsorb water loss within 1 hr upon being exposed to ambient air. This observation is consistent with results obtained by the above groups. Table IV shows the comparison of the lattice parameters obtained by several groups. There is some variation, which is probably due to the difference in water content and the preparation technique. The water molecules are believed to be on the 32*e* site as in $BaCdCl_6 \cdot 5H_2O$ (*30*).

The thermal stability of the sodium pyrochlore was studied with X-ray diffraction and DSC. X-ray studies showed that the pyrochlore phase remained stable up to 400°C and decomposed into a mixture of $Na_2W_4O_{13}$ and a few lines characteristic of $Na_2W_6O_{19}$. DSC data (Fig. 12) show two endothermic peaks and one small exotherm. The two endotherms correspond to the evolution of two different types of water in the structure. The possible water interactions are sodium–water, water–water, and oxygen–water from the WO_3 framework. Probably the most important interaction is the alkali ion–water one because this leads to the shortest bond distance.

TABLE IV

LATTICE PARAMETERS OF $WO_3 \cdot xH_2O$ PYROCHLORES

Lattice parameter (Å)	Cell size/W (Å^3)	Reference
10.278(2)	67.86	This work
10.305(3)	68.39	(*23*)
10.270(3)	67.70	(*25*)
10.206(3)	66.44	(*24*)

The energy needed to remove all the water from the structure is 27 kcal/mol. In the following discussion, we will examine the energy needed to remove the different waters that arise from the possible interactions within the lattice. The enthalpy values will be approximate because after the first exotherm (Fig. 12) there is no return to the original baseline, which would indicate where a peak begins and ends. This limits the accuracy of the ΔH values given. The first peak occurs at 480 K, and the enthalpy change is approximately 10 kcal/mol. This is similar to the value for $WO_3 \cdot xH_2O$ (*26*), and this endotherm corresponds to a zeolitic-type water loss that arises from the water–water inter-

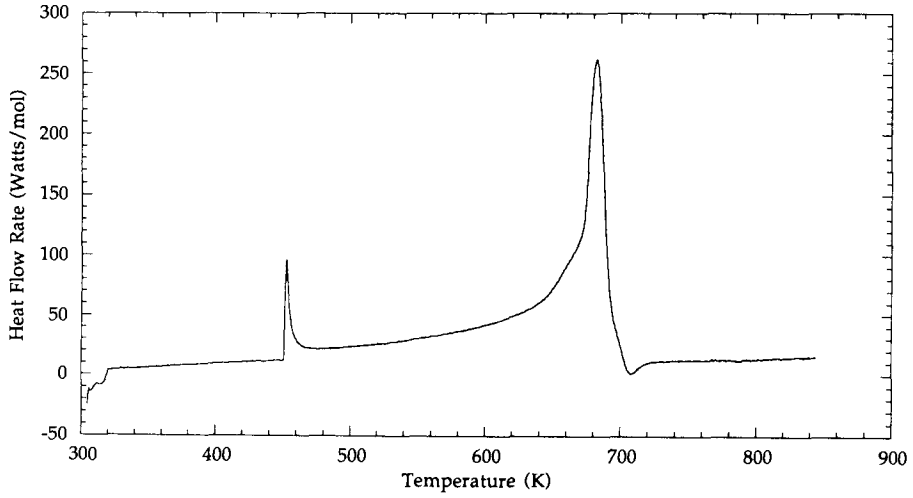

FIG. 12. DSC of the sodium pyrochlore phase at 10 K/min.

action. After the first endotherm, there is a broad endotherm from approximately 600 to 690 K that is due to the slow evolution of the second water. The sharp endotherm at 690 K is the bulk of the remaining water being removed, and the enthalpy change is roughly 17 kcal/mol. This dehydration is from the sodium–water interaction. This value is typical of zeolites and for the pyrochlore $KTaWO_6 \cdot H_2O$ (*31*). At 700 K (427°C), there is a small endotherm that corresponds to the decomposition of the pyrochlore structure. From the DSC data, which show that the endotherm comes immediately after the last of the water is removed, it appears that sodium pyrochlore is unstable unless there is a trace of water in the structure.

Intercalation Chemistry

By heating $WO_3 \cdot xH_2O$ pyrochlore to 300°C, we obtain pyrochlore WO_3 with empty tunnels. This empty pyrochlore is ideal for the ambient intercalation of lithium, sodium, potassium, and hydrogen. These topochemical insertion reactions of alkali metals into crystalline compounds have received much interest, due to their potential application in electrochromic devices and batteries. These reactions formally involve the reduction of the transition-metal ion with the charge being compensated by diffusion of the alkali metal, which donates an electron, into the host structure. Ideally only small structural changes occur upon insertion, which allows for the reaction to be reversed by oxidation. The compounds synthesized here provide an interesting set to determine the effect of structure on chemical reactivity.

Reaction of excess *n*-butyllithium with pyrochlore WO_3 and Na-pyrochlore led immediately to blue compounds that turn blue-black over several minutes. The compounds were allowed to equilibrate overnight to allow for the maximum lithium intercalation. Atomic absorption and back-titration of the excess *n*-butyllithium showed there was a range of intercalated lithium (Table V) from $0.7 \leq x \leq 1.0$. It is interesting that the empty pyrochlore and the pyrochlore with sodium and oxygen inside the three-dimensional tunnels both incorporate the same amount of lithium. This suggests that lithium does not reside on either the 8*b* or the smaller 16*d* site. Lithium probably pre-

TABLE V

LITHIUM INTERCALATION OF TUNGSTATES

Structure	Initial composition	Final composition	Lattice parameters (Å)	Cell size/W (Å^3)
Pyrochlore	WO_3	$Li_{0.7-1.0}WO_3$	a = 10.175(3)	65.84
Pyrochlore	$Na_{0.55}WO_{3.275}$	$Li_{0.7-1.0}Na_{0.55}WO_{3.275}$	a = 10.227(2)	66.85
Pyrochlore	$Ag_{0.55}WO_{3.275}$	$Li_{3.0}Ag_{0.55}WO_{3.275}$	a = 10.319(2)	68.67
Hexagonal	$Na_{0.3}WO_{3.15}$	$Li_{1.8-1.9}Na_{0.3}WO_{3.15}$	a = 7.446(2), c = 7.727(4)	61.84
Hexagonal	$Li_{0.20}WO_{3.10}$	$Li_{1.90}WO_{3.10}$	a = 7.441(3), c = 7.660(3)	61.22

fers one of the smaller sites in the structure. A contraction of the lattice might be expected to occur upon chemical intercalation of lithium because of the small size and the electropositive character of the lithium ion. The lattice parameter (Table V) does decrease to a = 10.175(3) Å from the 10.2395(9) Å of the empty pyrochlore structure. The chemical reversibility of the lithiation reaction was demonstrated by reaction with Br_2/CH_3CN mixture. The lithium was removed over a period of 1 week. The color went from blue-black to white, and X-ray studies showed that the sample was still a pyrochlore with similar lattice parameters as before the intercalation of lithium. Atomic absorption showed that a minute amount of lithium remained, about 0.02 Li/W. These compounds are now being studied electrochemically to determine the diffusion coefficient of the lithium, the long-term reversibility of the lithium, and the overall stability of these phases.

Lithiation of Ag-pyrochlore led immediately to a black compound. Lithium content was determined by back titration to be about 3.0Li/W, giving the chemical composition $Li_{6.0}Ag_{1.1}W_2O_{6.55}$. Other tungsten oxides have been shown to incorporate 2Li/W (*32*). In these compounds, the oxidation state of tungsten is between 3 and 4, which seems to be the lowest oxidation state of tungsten attainable upon intercalation. In the pyrochlore this accounts for four of the lithium. The rest of the lithium comes from the reduction of silver. Silver has a lower reduction potential than tungsten, so it should reduce before tungsten upon lithiation. It appears that the reduction of silver in the pyrochlore allows for greater intercalation than pyrochlore WO_3 with empty tunnels. X-ray studies of the phase indicated a single phase pyrochlore with a lattice contraction to 10.319 Å and no peaks for silver metal. This appears to indicate that silver metal stays inside the three-dimensional tunnels of the pyrochlore rather than precipitating out. Further work is being performed to locate the silver.

The reaction of *n*-butyl lithium with the Na-hexagonal compound leads immediately to a blue-black compound. Analysis showed that the lithium content ranges from $1.8 \leq x \leq 1.9$ per tungsten. This gives the general composition for the phase as $Li_{1.8-1.9}Na_{0.26}WO_{3.13}$. The amount of intercalated lithium is typical of the hexagonal tungsten bronzes with either empty tunnels or cations smaller than potassium located in the hexagonal cavity (*26, 32*). From structural considerations, empty hexagonal WO_3 could intercalate 1.0Li/W. The center of the hexagonal cavity can accommodate $\frac{1}{3}$ lithium, with $\frac{2}{3}$ lithium in the triangular prismatic site. Since many compounds contain more than one lithium, lithium must occupy a site(s) other than the most obvious ones in this structure. In our phase, sodium is most

likely in the hexagonal window; this site is not occupied in the fully reduced HTB compounds with the general formula M_xWO_3, with oxygen in the large cavity along the z axis. Some of the lithium is most likely on the 6*h* site, which is inside the triangular prismatic tunnel, as in $Li_yK_xWO_3$ (*33*). The remaining lithium must be in the hexagonal cavity with oxygen. On electrostatic grounds, this is a more reasonable assumption than having sodium in the hexagonal cavity surrounded by the positively charged lithium. There is ample room to fit both cations. The other scenario with lithium in the hexagonal window with either sodium or oxygen is not possible because there is room for only one atom. The lithiation is chemically reversible with a Br_2/CH_3CN solution over a period of 1 week. Atomic absorption showed that a residual amount of lithium was left in the structure, 0.02Li/W. The reaction of *n*-butyl lithium with $Li_{0.2}WO_{3.10}$, which also has the HTB structure, leads to the intercalation of lithium. In this compound, 1.7Li/W is incorporated into the lattice giving an overall composition $Li_{1.9}WO_{3.10}$. It appears that the maximum amount of lithium that can be intercalated into hexagonal WO_3 is approximately 2.0Li/W. The lattice parameters change dramatically upon lithiation (Table V): for sodium a = 7.446(4) Å and c = 7.727(5) Å, and for lithium a = 7.441(4) Å and c = 7.660(3) Å; in both cases a increases on lithium intercalation, c decreases, and the overall unit cell expands 1.5–3%, in contrast to the pyrochlore phase where an overall lattice contraction is observed.

These chemical-insertion reactions show that the degree of lithiation depends upon the structure of the host compounds and sometimes on the cation incorporated in the structure. These insertion reactions allow for the formation of reduced novel tungsten compounds that may hold some promise in electrochromic displays. The chemical insertion of sodium, potassium, and hydrogen into these compounds has also been accomplished and will be published shortly. Electrochemical studies are now underway to determine the feasibility of the use of these compounds in electrochromic displays.

Conclusion

We have shown that low-temperature hydrothermal synthesis of various tungstates leads to the formation of both pyrochlore and hexagonal tungsten bronze phases. Both phases incorporate cations along with oxygen and water inside the tunnels. The cations in these structures can be exchanged for other monovalent cations. The phases are metastable and cannot be prepared via traditional high-temperature solid-state synthetic techniques.

Acknowledgments

We gratefully acknowledge the financial support from NSF under grant DMR-8913849. We thank Max Budd of the Geology Department for the AA measurement, and Mary Patt and Professor E. Cotts of the Physics Department for making the DSC measurements.

References

1. M. S. WHITTINGHAM, *in* "Solid State Devices" (B. V. R. Chowdari and S. Radhakrishna, Eds.), World Scientific, Singapore (1988).
2. K. P. REIS, A. RAMANAN, AND M. S. WHITTINGHAM, *Chem. Mater.* **2,** 219 (1990).
3. M. S. WHITTINGHAM, *in* "Recent Advances in Fast Ion Conducting Materials and Devices" (B. V. R. Chowdari, Q. Liu, and L. Chen, Eds.), p. 179, World Scientific, Singapore (1990).
4. B. GERAND, G. NOWOGROCKI, J. GUENOT, AND M. FIGLARZ. *J. Solid State Chem.* **29,** 429 (1979).
5. D. BABEL, G. PAUSEWANG, AND W. VIEBAHN, *Z. Naturforsch.* **22b,** 1219 (1967).
6. A. W. SLEIGHT, F. C. ZUMSTEG, J. R. BARKLWY, AND J. E. GULLEY, *Mater. Res. Bull.* **13,** 1247 (1978).
7. M. A. SUBRAMANIAN, G. A. ARVAMUELAN, G. V. SUBBA RAO, *Prog. Solid State Chem.* **15,** 55 (1983).
8. R. A. BEYERLEIN, H. S. HOROWITZ, J. M. LONGO, AND M. E. LENOWICZ, *J. Solid State Chem.* **51,** 253 (1984).

9. M. A. SUBRAMANIAN, A. CLEARFIELD, A. M. UMARJI, G. K. SHENOY, AND G. V. RAO, *J. Solid State Chem.* **52,** 124 (1984).
10. K. P. REIS, A. RAMANAN, W. GLOFFKE, AND M. S. WHITTINGHAM, *Mater. Res. Soc. Symp. Proc.* (*Solid State Ionics II*) **210,** 473 (1991).
11. K. P. REIS, E. PRINCE, AND M. S. WHITTINGHAM, to be published.
12. M. POPE, "Heteropoly and Isopoly Oxometallates," Springer-Verlag, New York/Berlin (1983).
13. A. MAGNÉLI, *Acta Chem. Scand.* **7,** 315 (1953).
14. T. A. BITHER, J. L. GILLSON, AND H. S. YOUNG, *Inorg. Chem.* **5,** 1559 (1966).
15. T. E. GIER, D. C. PEASE, A. W. SLEIGHT, AND T. A. BITHER, *Inorg. Chem.* **6,** 1646 (1968).
16. K. H. CHENG, A. J. JACOBSON, AND M. S. WHITTINGHAM, *Solid State Ionics* **1,** 15 (1980).
17. B. GERAND, G. NOWOGROCKI, AND M. FIGLARZ, *J. Solid State Chem.* **38,** 312 (1981).
18. M. LEBLANC, G. FEREY, P. CHEVALLIER, Y. CALAGE, AND R. DE PAPE, *J. Solid State Chem.* **47,** 53 (1983).
19. M. SUZUKI, N. WADA, D. R. HINES, AND M. S. WHITTINGHAM, *Phys. Rev.* **36,** 2844 (1987).
20. P. G. DICKENS AND S. A. KAY, *Solid State Ionics* **8,** 291 (1983).
21. M. V. SUSIC AND Y. M. SOLONIN, *J. Mater. Sci.* **23,** 267 (1988).
22. R. C. T. SLADE, B. C. WEST, AND G. P. HILL, *Solid State Ionics* **32/33,** 154 (1989).
23. J. R. GÜNTER, M. AMBERG, AND H. SCHMALLE, *Mater. Res. Bull.* **24,** 289 (1989).
24. R. NEDJAR, M. M. BOREL, M. HERVIEU, AND B. RAVEAU, *Mater. Res. Bull.* **23,** 91 (1988).
25. A. COUCOU, AND M. FIGLARZ, *Solid State Ionics* **28–30,** 1762 (1989).
26. M. FIGLARZ, *Prog. Solid State Chem.* **19,** 1 (1989).
27. D. W. MURPHY, R. J. CAVA, K. RHYNE, R. S. ROTH, A. SANTORO, S. M. ZAHURAK, AND J. L. DYE, *Solid State Ionics* **18–19,** 799 (1986).
28. A. CLEARFIELD, *Chem. Rev.* **88,** 125 (1988).
29. M. ABE, *J. Inorg. Nucl. Chem.* **41,** 85 (1979).
30. M. LEDESAT AND B. RAVEAU, *J. Solid State Chem.* **67,** 340 (1987).
31. C. M. MARI, M. CATTI, AND A. CASTILLE, *Mater. Res. Bull.* **21,** 773 (1986).
32. K. H. CHENG, A. J. JACOBSON, AND M. S. WHITTINGHAM, *Solid State Ionics* **5,** 355 (1981).
33. R. C. T. SLADE, B. C. WEST, A. RAMANAN, W. I. F. DAVID, AND W. T. A. HARRISON, *Eur. J. Solid State Inorg. Chem.* **26,** 15 (1989).